EPJ Web of Conferences **95**, 04067 (2015)
DOI: 10.1051/epjconf/20159504067

Open heavy flavor measurements at STAR

David Tlustý[1,a]

[1] *Nuclear Physics Institute, ASCR*

Abstract. In relativistic heavy ion collisions at RHIC, heavy quarks are expected to be created from initial hard scatterings. Since heavy quarks have large masses, long life time, and negligible annihilation due to their small population, the number of heavy quarks is conserved during whole medium evolution. The interaction between heavy quarks and the medium is sensitive to the early medium dynamics, therefore heavy quarks are suggested as an ideal probe to quantify the properties of the strongly interacting QCD matter.
In this article, we report on recent STAR results of open heavy flavor production at $\sqrt{s}$ = 200 and 500 GeV in p+p, $\sqrt{s_{NN}}$ = 200 GeV in Au+Au and $\sqrt{s_{NN}}$ = 193 GeV in U+U collisions.

1 Introduction

In relativistic heavy ion collisions at RHIC, heavy quarks are expected to be created from initial hard scatterings. Since heavy quarks have large masses, long life time, and negligible annihilation due to their small population, the number of heavy quarks is conserved during whole medium evolution. The interaction between heavy quarks and the medium is sensitive to the medium properties, such as the transport coefficients, during its early stages when the QGP phase is expected to exist in heavy-ion collisions [1].

Energetic heavy quarks were predicted to lose less energy than light quarks via gluon radiation when they traverse the QGP owing to the "Dead cone effect" [2]. In contrast, measurements [3–5] show significant suppression at high transverse momentum, p_T, in central heavy ion collisions, similar to that of light hadrons. This has led to the reconsideration of the effect of heavy-quark collisional energy loss [6, 7].

Heavy quarks are expected to hadronize in elementary collisions mainly through hard fragmentation. In high-energy heavy-ion collisions, the large charm-pair abundance could increase the coalescence probability, in particular for $p_T < 2$ GeV/c. The coalescence of charm with a light quark from the medium with a large radial flow may introduce a p_T-dependent enhancement to the observed charmed hadron spectrum compared to that from fragmentation [23, 24]. Furthermore, this may lead to a baryon-to-meson enhancement for charmed hadrons similar to that observed for light-flavor hadrons [25, 27].

The state-of-art measurements of inclusive heavy quark production are carried out through two main approaches:

[a] e-mail: tlusty@gmail.com

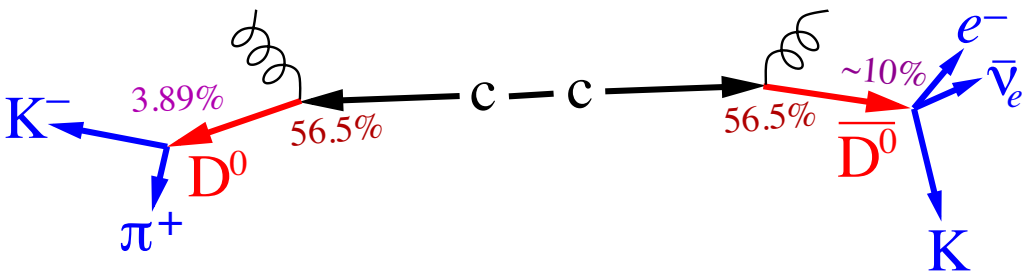

Figure 1. Charm quark fragmentation to D^0 and two main D^0 decay channels.

1. single electrons from open heavy hadron semi-leptonic decays
2. hadrons from hadronic decays

Both are drawn schematically in Fig. 1 which depicts a created pair of charm quarks hadronizing into D^0 and $\overline{D^0}$ with the probability of 56.5%. The figure further shows the D^0 undergoing a hadronic decay into negative kaon and positive pion with branching ratio of 3.87% and $\overline{D^0}$ undergoing a semi-leptonic decay electron, corresponding neutrino and a kaon. The branching ratios as well as the hadronization probability are taken from Ref. [12]. The first approach provides an abundant statistics owing to the variety of decay channels in which those electrons called non-photonic electrons (NPE) are created. The second approach provides direct access to open charm meson kinematics owing to the possibility of the D^0 invariant mass reconstruction and allows to distinguish an open charm hadron from others.

2 Analysis Method and Datasets

Invariant yield of charm quark production dY is calculated as

$$dY \equiv \frac{\mathrm{d}^2 N_{c\bar{c}}}{2\pi p_T \mathrm{d}p_T \mathrm{d}y} = \frac{1}{N_{\mathrm{trig}}} \frac{Y(p_T, y)}{2\pi p_T \Delta p_T \Delta y} \frac{f_{\mathrm{trg}}}{\Gamma \, f_{\mathrm{frag}} \epsilon_{\mathrm{rec}}} \tag{1}$$

where N_{trig} is the total number of triggered events used for the analysis. $Y(p_T, y)$ is the raw charm hadron signal in each p_T bin within a given rapidity window Δy. Γ is the hadronic decay branching ratio for the channel of interest. ϵ_{rec} is the reconstruction efficiency including geometric acceptance, track selection efficiency, particle identification (PID) efficiency, and analysis cut efficiency. f_{frag} represents the the ratio of charm quarks hadronized to open charm mesons. And f_{trg} is the correction factor to account for the trigger bias. f_{trg} is found to be unity in Au+Au, 0.65 in p+p collisions at $\sqrt{s}$ = 200 GeV and 0.58 in p+p collisions at $\sqrt{s}$ = 500 GeV.

$Y(p_T, y)$ is obtained from fitting the invariant mass spectrum (Fig. 2) of open charm mesons through hadronic decays: $D^0(\overline{D^0}) \rightarrow K^{\mp}\pi^{\pm}$ (Γ = 3.89%) and $D^{*\pm} \rightarrow D^0(\overline{D^0})\pi^{\pm}$ (Γ = 67.7%) $\rightarrow K^-\pi^+\pi^{\pm}$ (total Γ = 2.63%)

The daughter particles were identified by Time Projection Chamber (TPC) and Time-Of-Flight (TOF) subsystems of the STAR experiment [15] at mid-rapidity $|y| < 1$ at $\sqrt{s_{NN}}$ = 200 and 500 GeV.

In years 2009-2012, STAR did not have the capability to reconstruct the secondary vertex of D^0 decay; one had to calculate the invariant mass of all $K\pi$ pairs coming from the vicinity of the primary

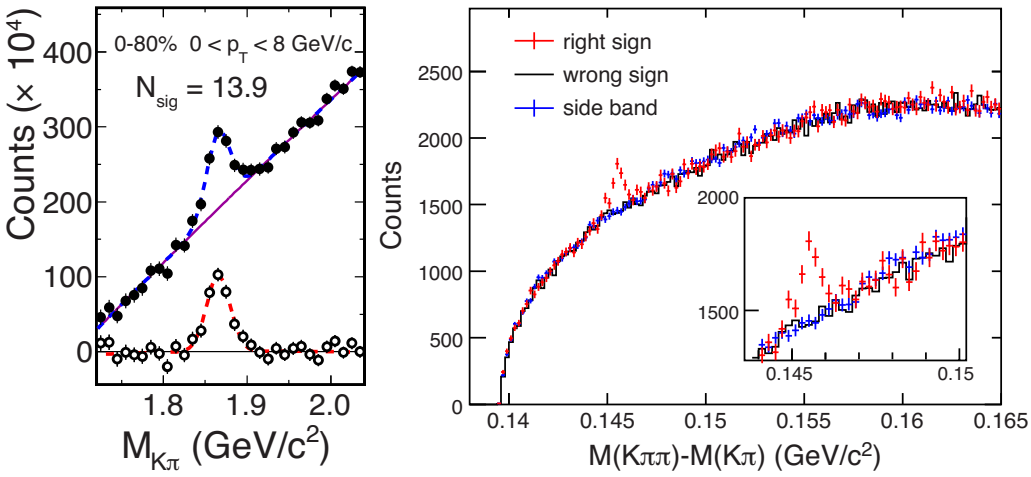

Figure 2. Left panel: D^0 signal in Au+Au 200 GeV collisions after mixed-event background subtraction. Figure taken from Ref. [13]. Right panel: D^* signal in p+p 200 GeV collisions with combinatorial background reproduced by wrong-sign and side-band methods [14].

vertex. This results in a large combinatorial background which was reconstructed via the mixed-event method (Au+Au dataset), same-charge-sign, and kaon momentum-rotation (p+p dataset) and subtracted from invariant mass spectra of all particle pairs [16]. The $D^{*\pm}$ meson undergoes a cascading decay

$$D^{*\pm} \xrightarrow[p^*=39\ \mathrm{MeV/c}]{B.R.=67.7\%} D^0\pi_S^{\pm} \xrightarrow{B.R.=3.89\%} K^{\mp}\pi^{\pm}\pi_S^{\pm}$$

with very low decay energy giving both daughter particles momentum in CMS of 39 MeV/c. Hence the difference in invariant mass

$$\Delta M \equiv (M_{K^{\mp}\pi^{\pm}\pi^{\pm}} - M_{K^{\mp}\pi^{\pm}}; 1.84 < M_{K^{\mp}\pi^{\pm}} < 1.89\ \mathrm{GeV}/c^2)$$

has very low combinatorial background around 145.4 MeV/c^2, which is the difference in mass of the $D^{*\pm}$ and the D^0 meson, and whose resolution is determined by mostly the soft pion π_S momentum resolution. Both factors imply the ability to have a significant peak in ΔM spectrum around 145.4 MeV/c^2.

The combinatorial background was reconstructed by side-band (picking $K\pi$ pair outside the D^0 mass region) and wrong-sign (picking soft pion with opposite charge) methods. The dominant source of systematic uncertainties for both D^0 and D^* analyses was the difference between yields obtained from subtractions of combinatorial background from all particle combinations.

3 Results

3.1 D Meson Production in p+p Collisions

Yields $Y(p_T, y)$ were calculated in p_T bins and the charm cross section at mid-rapidity $\mathrm{d}\sigma^{c\bar{c}}/\mathrm{d}y$ was obtained from the power-law function

$$f_{\mathrm{Hagedorn}}(p_T, y) = 4\frac{\mathrm{d}\sigma^{c\bar{c}}}{\mathrm{d}y}\frac{(n-1)(n-2)}{\langle p_T\rangle^2(n-3)^2}\left(1+\frac{2p_T}{\langle p_T\rangle(n-3)}\right)^{-n} \quad (2)$$

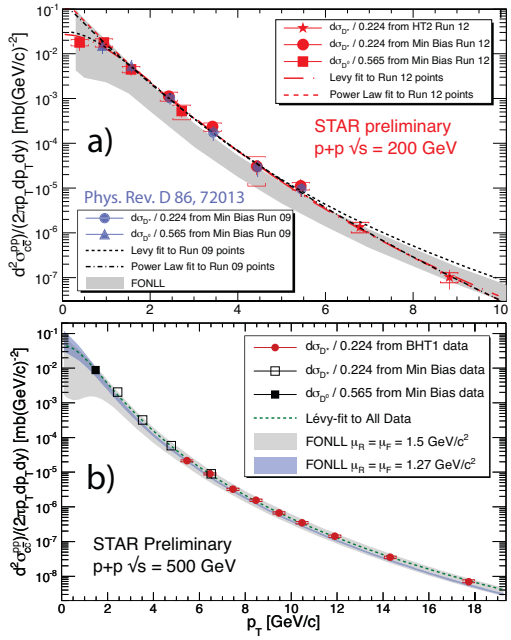

Figure 3. Charm quark production cross section as inferred from D^0 and D^* production in p+p collisions at $\sqrt{s}$ =200 GeV (panel a) and at $\sqrt{s}$ =500 GeV (panel b) compared with FONLL prediction (shaded bands).

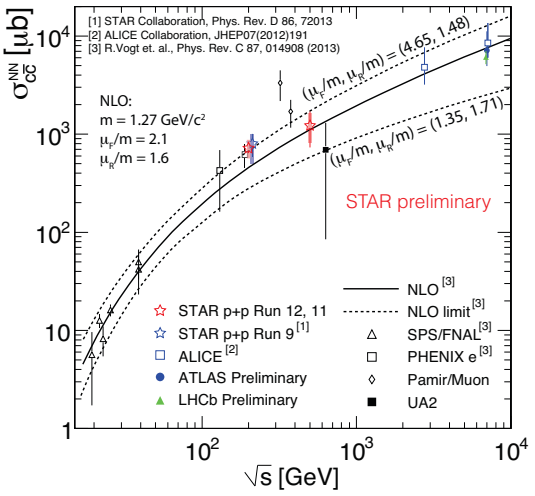

Figure 4. Total charm cross section as a function of $\sqrt{s}$.

or

$$f_{\mathrm{Levy}}(p_T, y) = \frac{\mathrm{d}\sigma_{c\bar{c}}}{\mathrm{d}y} \frac{(n-1)(n-2)}{2\pi nC[nC + m_0(n-2)]} \left(1 + \frac{\sqrt{p_T^2 + m_0^2} - m_0}{nC}\right)^{-n} \tag{3}$$

fit [14] to $\mathrm{d}^2\sigma^{c\bar{c}}/(2\pi p_T \mathrm{d}p_T \mathrm{d}y) = dY \cdot \sigma_{\mathrm{NSD}}$, where dY was obtained from (1). σ^{NSD} is the total non-single diffractive (NSD) cross section, which is measured at STAR to be 30.0 ± 2.4 mb at $\sqrt{s}$ = 200 GeV [17]. In the case of $\sqrt{s}$ = 500 GeV, there is no STAR measurement yet; σ^{NSD} is extrapolated from 200 GeV measurement with the help of PYTHIA simulation to be 34 mb.

STAR has published results on $\frac{\mathrm{d}^2\sigma^{c\bar{c}}}{2\pi p_T \mathrm{d}p_T \mathrm{d}y}$ for $0.6 < p_T < 6$ GeV/c in p+p collisions at $\sqrt{s}$=200 GeV [14]. The measurement was done on minimum-bias-triggered (MB) events with data taken in 2009. Recently, a new measurement has been carried out using data taken in p+p collisions at $\sqrt{s}$=200 GeV in 2012, with both MB events and events triggered on energy deposition in a Barrel ElectroMagnetic Calorimeter (BEMC) tower above certain thresholds, i.e., High-E_T triggers (HT). The HT results, after correcting for the trigger efficiency, are consistent with the MB results in the overlapping p_T region. As can be seen in panel a) of Fig. 3, the new analysis extends the p_T range down to 0 GeV/c, thanks to the larger MB data sample size, and up to 10 GeV/c, owing to the inclusion of the HT data sample. These new results are consistent with the published ones, and in agreement with fixed order, next-to-leading logarithm (FONLL) pQCD calculations [18]. A similar analysis has also been done using data taken in p+p collisions at $\sqrt{s}$=500 GeV, with both MB and HT events. The charm

production cross section is measured as a function of p_T for $1 < p_T < 20$ GeV/c. The results are consistent with the latest FONLL calculations [19], as shown in panel b) of Fig. 3.

In order to compare STAR results with other experiments, we extrapolated $\left.\frac{\mathrm{d}\sigma_{c\bar{c}}}{\mathrm{d}y}\right|_{y=0}$ to $\sigma_{c\bar{c}}$ using PYTHIA simulations with various parameter tunings giving extrapolation factors 4.7 ± 0.7 for 200 GeV and 5.6 ± 0.1 for 500 GeV collisions. The results are shown in Fig. 4.

3.2 D^0 Production in Heavy Ion Collisions

Yields $Y(p_T, y, N_{\mathrm{bin}})$ were calculated in p_T and centrality bins. The charm pair per nucleon-nucleon-collision production cross section $\mathrm{d}\sigma^{\mathrm{NN}}_{c\bar{c}}/\mathrm{d}y$ was obtained from the integral of

$$\frac{\mathrm{d}^2\sigma^{\mathrm{NN}}_{c\bar{c}}}{2\pi p_T \mathrm{d}p_T \mathrm{d}y} = dY \cdot \frac{\sigma^{\mathrm{inel}}}{N_{\mathrm{bin}}} \tag{4}$$

over p_T and is measured to be $\left.\frac{\mathrm{d}\sigma^{\mathrm{NN}}_{c\bar{c}}}{\mathrm{d}y}\right|_{y=0} = 175 \pm 13(\mathrm{stat.}) \pm 23(\mathrm{sys.})\ \mu\mathrm{b}$. We assumed the same $f_{\mathrm{frag}}(0.565 \pm 0.032)$ as in p+p collisions. dY is obtained from (1) and $\sigma^{\mathrm{inel}} = 42$ mb is the total inelastic cross section [20]. The N_{bin} is the number of binary collisions. $\mathrm{d}\sigma^{\mathrm{NN}}_{c\bar{c}}/\mathrm{d}y|_{y=0}$ as a function of N_{bin} is shown in the right panel of Fig. 6. Within errors, the results are in agreement and follow the number-of-binary-collisions scaling, which indicates that charm quark is produced via initial hard scatterings at early stage of the collisions at RHIC.

Differences in the kinematic distributions of particles between high-energy heavy-ion collisions and p+p collisions can be quantified by the nuclear modification factor R_{AA} whose deviation from unity carries information about the properties of the QGP and its interaction with particles under study. The R_{AA} was calculated as

$$R_{\mathrm{AA}}(p_T, N_{\mathrm{bin}}) = \frac{dY(p_T, N_{\mathrm{bin}})}{N_{\mathrm{bin}} f_{\mathrm{Levy}}(p_T)} \tag{5}$$

where the $f_{\mathrm{Levy}}(p_T)$ represents the p+p reference. $dY(p_T, N_{\mathrm{bin}})$ together with $N_{\mathrm{bin}} f_{\mathrm{Levy}}(p_T)$ are shown in the left panel of Fig. 5 and $R_{\mathrm{AA}}(p_T, y)$ in panels a), b), and c) of Fig. 5 corresponding to different N_{bin} revealing strong suppression in the most central collisions for $p_T > 2$ GeV/c. Our $R_{\mathrm{AA}}(p_T)$ are compared to various model calculations1 [21–25]. We find that model calculations including a substantial amount of charm-medium interaction and hadronization through both fragmentation and coalescence can describe the data. The charm-medium interaction is needed for the suppression at large p_T, while coalescence could be important for the enhancement at p_T around 1.3 GeV/c.

More recently, STAR has measured R_{AA} of D^0 meson in U+U collisions at $\sqrt{s_{\mathrm{NN}}} = 193$ GeV, where the Bjorken energy density is predicted to be about 20% higher than that in the same centrality interval in Au+Au collisions [26]. The suppression of D^0 meson production at large p_T in Au+Au and U+U collisions follows a global trend as a function of the number of participant nucleons in the collisions, $\langle N_{\mathrm{part}} \rangle$ and is consistent with that measured for $\pi^{\pm}$, as can be seen in the left panel of Fig. 6.

4 Conclusions and Outlook

STAR has measured open heavy-flavor production in p+p, Au+Au and U+U collisions. The measured production cross sections of charm quarks in p+p collisions are consistent with perturbative QCD calculations. Model calculations including a substantial amount of charm-medium interaction

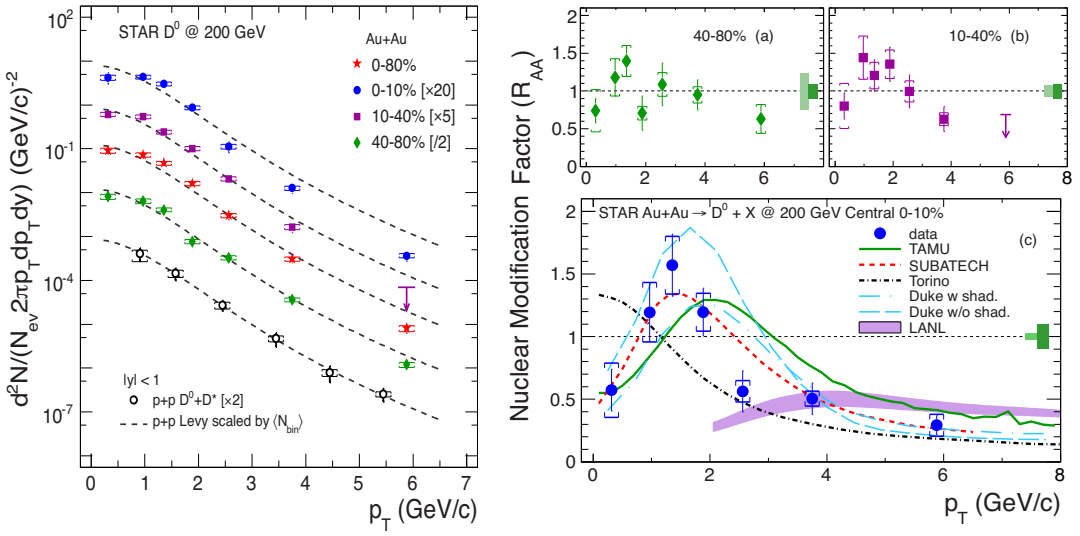

Figure 5. Left Panel: Centrality dependence of the D^0 p_T differential invariant yield in Au+Au collisions (solid symbols). The curves are number-of-binary-collision-scaled Levy functions from fitting to the p+p result (open circles) [14]. The arrow denotes the upper limit with 90% confidence level of the last data point for 10-40% collisions. The systematic uncertainties are shown as square brackets. Right panel: D^0 nuclear modification factor $R_{\rm AA}$ as a function of p_T for most peripheral (panel a), semi-central (panel b), and the most central (panel c) Au+Au collisions with theoretical predictions [21–25]. Green rectangles around unity represent systematic uncertainties of $N_{\rm bin}$ uncertainty and p+p normalization error.

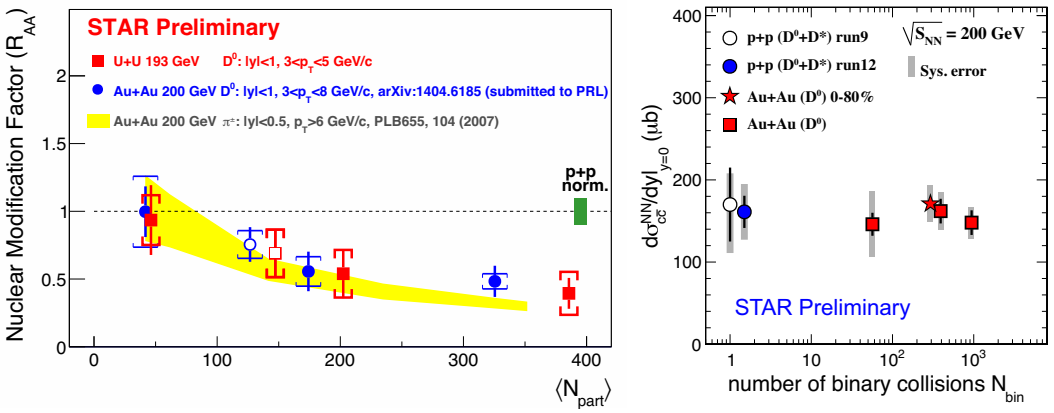

Figure 6. Left Panel: Nuclear modification factor $R_{\rm AA}$ as a function of the number of participant nucleons $\langle N_{\rm part}\rangle$ in Au+Au or U+U collisions for D^0 with $p_T > 3$ GeV/c. Right panel: The charm production cross section per $N_{\rm bin}$ as a function of $N_{\rm bin}$.

and hadronization via both fragmentation and coalescence describe the measured D^0 meson nuclear modification factor $R_{\rm AA}$. STAR has been recently upgraded with two new detectors, the Heavy Flavor Tracker (HFT) [27] and Muon Telescope Detector (MTD) [28]. The HFT is based on cutting-edge silicon detector technologies with excellent position resolutions and low material budgets. It provides STAR with the capability of identifying heavy-flavor particles and distinguishing between charm and bottom on an event-by-event basis through track impact parameter measurements [29]. The MTD enables STAR to identify high-p_T muons for the first time, which is important for quarkonium measurements in di-muon decay channels and for open heavy-flavor measurements through e. g. electron-muon correlations. With the additions of the HFT and MTD, STAR is in an excellent position for heavy-flavor measurements with unprecedented precision in the coming years.

Acknowledgements

This work has been supported by the grant 13-02841S of the Czech Science Foundation (GACR) and by the Grant Agency of the Czech Technical University in Prague,
grant No. SGS13/215/OHK4/3T/14.

References

[1] B. Muller, Nucl. Phys. A **750**, 84 (2005)
[2] Yu. L. Dokshitzer and D.E. Kharzeev, Phys. Lett. B **519**, 199 (2001)
[3] B. I. Abelev *et al.*, Phys. Rev. Lett. **98**, 192301 (2007)
[4] S. S. Adler *et al.*, Phys. Rev. Lett. **96**, 032301 (2006)
[5] B. I. Abelev *et al.*, J. High Energy Phys. **09**, 112 (2012)
[6] M. Djordjevic, M. Gyulassy and S. Wicks, Phys. Rev. Lett. **94**, 112301 (2005)
[7] A. Adil and I. Vitev, Phys. Lett. B **649**, 139 (2007)
[8] He *et al.*, Phys. Rev. C **86**, 014903 (2012)
M. He *et al.*, Phys. Rev. Lett. **110**, 112301 (2013)
[9] P. B. Gossiaux *et al.*, J. Phys. G **37**, 094019 (2010)
P. B. Gossiaux *et al.*, Nucl. Phys. A **904-905**, 992c (2013)
[10] B. I. Abelev *et al.*, Phys. Rev. C **75**, 064901 (2007)
[11] B. I. Abelev *et al.*, Phys. Rev. Lett. **97**, 152301 (2006)
[12] J. Beringer *et al.*, Phys. Rev. D **86**, 010001 (2012)
[13] L. Adamczyk *et al.*, Phys. Rev. Lett. **113**, 72301 (2014)
[14] L. Adamczyk *et al.*, Phys. Rev. D **86**, 072013 (2012)
[15] M. Shao *et al.*, Nucl. Instrum. Methods A **499**, 624 (2003).
[16] J. Adams *et al.*, Phys. Rev. Lett. **94**, 062301 (2005).
[17] J. Adams *et al.* [STAR Collaboration], Phys. Rev. Lett. **91**, 172302 (2003)
[18] M.Cacciari, P.Nason, and R.Vogt, Phys. Rev. Lett. **95**, 122001 (2005)
[19] R. Vogt, private communication, (2012).
[20] M. Honda *et al.*, Phys. Rev. Lett. **70**, 525 (1993)
[21] M. He, R. J. Fries, R. Rapp, arXiv: 1204.4442.
[22] P. B. Gossiaux, J. Aichelin, M. Bluhm, T. Gousset, M. Nahrgang, S. Vogel, K. Werner, arXiv: 1207.5445.

[23] W. M. Albericoetal., Euro. Phys. J **71**, 1666 (2011)
W. M. Albericoetal., Euro. Phys. J.**73**, 2481 (2013)
[24] S. S. Cao, G. Y. Qin and S. A. Bass, Phys. Rev. C **88**, 044907 (2013)
[25] R. Sharma, I. Vitev and B. W. Zhang, Phys. Rev. C **80**, 054902 (2009)
[26] D. Kikola, G. Odyniec and R. Vogt, Phys. Rev. C **84**, 054907 (2011)
[27] Technical Design Report: The STAR Heavy Flavor Tracker (2011)
[28] L. Ruan *et al.*, J. Phys. G: Nucl. Part. Phys. **36**, 095001 (2009)
[29] Y.Zhang *et al.*, J. Phys. G: Nucl. Part. Phys. **41**, 025103 (2014)